NASA Contractor Report 172273

ICASE

SPINNING MODE ACOUSTIC RADIATION FROM THE FLIGHT INLET

William F. Moss

Contract Nos. NAS1-16394 and NAS1-17130
November 1983

INSTITUTE FOR COMPUTER APPLICATIONS IN SCIENCE AND ENGINEERING
NASA Langley Research Center, Hampton, Virginia 23665

Operated by the Universities Space Research Association

National Aeronautics and
Space Administration

Langley Research Center
Hampton, Virginia 23665

SPINNING MODE ACOUSTIC RADIATION FROM THE FLIGHT INLET

William F. Moss
Clemson University

ABSTRACT

A mathematical model has been developed for spinning mode acoustic radiation from a thick wall duct without flow. This model is based on a series of experiments (with and without flow) conducted by Richard Silcox [Silcox] of the Noise Control Branch at Langley Research Center. In these experiments a nearly pure azimuthal spinning mode was isolated and then reflection coefficients and far field pressure (amplitude and phase) was measured. In our model the governing boundary value problem for the Helmholtz equation is first converted into an integral equation for the unknown acoustic pressure over a disk, S1, near the mouth of the duct and over the exterior surface, S2, of the duct. Assuming a pure azimuthal mode excitation, the azimuthal dependence is integrated out which yields an integral equation over the generator C1 of S1 and the generator C2 of S2 (see Figure 2). We approximate the sound pressure on C1 by a truncated modal expansion of the interior acoustic pressure. We use piecewise linear spline approximation on C2. We collocate at the knots of the spline and at zeros of the first term excluded in the truncated modal expansion. Finally, we compare numerical and experimental results.

Research was supported by the National Aeronautics and Space Administration under NASA Contracts No. NAS1-17130 and NAS1-16394 while the author was in residence at the Institute for Computer Applications in Science and Engineering, NASA Langley Research Center, Hampton, VA 23665.

INTRODUCTION

The reduction of jet noise radiated from the inlets of aircraft engines has become an increasing important problem. Methods to suppress this noise have included the development of acoustic liners, high Mach number inlets, and the use of inlet geometry to redirect the sound. Experiments with and without flow have been conducted at Langley Research Center [Ville], [Silcox] to study these methods. In particular, in July 1982 an experimental study was conducted by Richard Silcox [Silcox] in a continuing effort to examine the effect of inlet geometry on the reflected and radiated acoustic fields.

This report describes a mathematical model for the no-flow experiments. This model has been constructed to cover a range of reduced wave numbers and azimuthal and radial modes. The inlet contour can be modified so that the result is a model for both inlet and engine, each with its own excitation. An axisymmetric impedance boundary condition can also be easily incorporated into a portion of the interior duct wall.

The experiments of Richard Silcox were designed around the spinning mode synthesizer (SMS) in the Langley Research Center flow duct facility. The SMS can excite a nearly pure (20-30 dB isolation) azimuthal mode inside the duct. This modal expansion for the interior acoustic pressure is built into the model. At an artificial circular disk interface, S1, near the mouth of the duct, the pressure and its normal derivative are required to match continuously (see Figure 2). On the exterior duct surface, S2, a hard wall boundary condition is imposed. In the exterior region, the pressure is required to satisfy the Helmholtz equation and the radiation condition at infinity. This boundary value problem is converted into an integral equation over S1 + S2 using Helmholtz' formula. The unknowns in this equation are

the complex pressure on S2 and the reflection coefficients in the interior modal expansion.

By assuming a single azimuthal mode excitation, it is possible to integrate out the azimuthal dependence which yields an integral equation over the generator C1 + C2 of S1 + S2. We arrive at a one-dimensional integral equation at the expense of a somewhat more complicated kernel.

The numerical method used is collocation; i.e., the integral equation is required to be satisfied at certain points on C1 + C2. The unknown pressure on C1 (and its normal derivative) is approximated by a finite Bessel series which is a truncation of the interior azimuthal mode expansion. Piecewise linear spline approximation is used on C2. The absolute error in the solution is estimated at the knots of the spline and this information is used to recommend the number of knots required for a given error tolerance on C2. This information can also be used to distribute the recommended number of knots to achieve an equal distribution of the absolute error. This is useful if it should be necessary to run the code a second time in order to achieve a better error performance. The code also provides (optionally) for one step of Neumann iteration. This yields a natural interpolation formula for the pressure, and gives an approximation with the same smoothness as the exact solution. Finally, Helmholtz' formula is used to compute the pressure on a semicircle in front of the duct for comparison with experimental results.

In Section 2 we give for completeness a brief description of the SMS and the Langley Research Center flow duct facility. In Section 3 we describe the mathematical details of the model, while in Section 4 we outline the numerical method. Our codes and their implementation are discussed in Section 5. Numerical results are presented in Section 6 and Section 7 contains concluding remarks.

2. THE SPINNING MODE SYNTHESIZER (SMS)

For completeness, we give a brief description of the SMS. The reader is referred to Figure 1 and references [Pal] and [Ville]. The following is taken from [Ville].

The SMS incorporated into the flow duct facility is a research apparatus designed to overcome the problems involved in static testing of real turbofan engines or research fans. The SMS generates arbitrary combinations of acoustic patterns at a specified frequency in a 0.3 meter duct (with or without airflow). Specified duct modes are generated by controlling the amplitude and phase of 24 acoustic drivers equispaced around the duct wall in a plane perpendicular to the duct center line. By properly adjusting the input to the drivers, individual spinning modes, a combination of modes, or circumferential standing waves can be generated in the duct. The acoustic field produced by the array of drivers is monitored by an array of 48 wall mounted microphones located 0.2 meters upstream of the drivers. At these microphone locations the desired acoustic wall pressures (amplitude and phase) are approximated to some specified degree of accuracy. In order to attain this accuracy, the pressure field sensed by the 48 microphones feeds back through a control computer optimization algorithm to generate correction signals to the drivers. By an iterative process, the pressure field at the microphone array converges to some specified target pressure at the monitoring array. Once the target pressure is attained, the mode setup may be stored by recording the driver settings for future recall, or the steady state acoustic field may be left intact for experimental studies.

The inlet duct test apparatus is mounted in the flow duct facility of the Langley Aircraft Noise Reduction Laboratory and extends into the anechoic

chamber shown by the view in Figure 1. This chamber measures 9.15 meters wide, by 6.1 meters deep by 7.16 meters high.

The flight inlet is attached to the inlet section of the duct. The geometry actually used in our model is indicated in Figure 2. We have extended the flight inlet contour BCD with a straight (r = constant) portion DE, and quarter arc of a circle EF. We note that our numerical results indicate that this termination of the inlet has little effect at the frequencies considered.

3. THE MODEL

This model was suggested by the approach of Kagawa, et al. [Kag] to loudspeaker design.

Figure 2 gives a contour drawing of the idealized inlet. This is the flight inlet contour (an arc BC of an ellipse plus the line segment CD) with a straight extension DE and a quarter circle termination EF.

Let a denote the interior duct radius ($a = 0.15$ meters) and introduce a cylindrical coordinate system $(\bar{z},\bar{r},\theta)$ with origin 0 and positive $\bar{z}$ axis pointing out of the duct. Let ω denote angular frequency, c the speed of sound, and $\bar{k} = \omega/c$ the reduced wave number. We will use the dimensionless coordinates $z = \bar{z}/a$ and $r = \bar{r}/a$ and the parameter $k = \bar{k}a$. Let Ω denote the exterior of S1 + S2 and let D denote the interior of S1 + S2.

We denote complex pressure by $\Phi(z,r,\theta)e^{-i\omega t}$ where

$$\Phi = \begin{cases} \phi, & -d \leq z \leq 0, \quad r \leq 1 \\ \psi, & \text{in } \Omega \end{cases} .$$

For a fixed integer m, it is assumed that the SMS generates the modal expansion $\phi = \bar{\phi} e^{im\theta}$ with

$$\bar{\phi} = \sum_{n=0}^{\infty} \left(A(n)e^{iL(n)z} + R(n)e^{-iL(n)z}\right) J_m(\lambda(n)r). \tag{3.1}$$

This expansion comes from separation of variables in the reduced wave equation plus application of the hard wall boundary condition. In practice other "m" or azimuthal modes are present inside the duct but are at least 20 dB below the desired mode. In (3.1) J_m denotes the ordinary Bessel function of the first kind and order m. The increasing sequence $\lambda(n)$ is defined by $J_m'(\lambda(n)) = 0$, $n \geq 0$. We assume that $k \neq \lambda(n)$ for all n and define NCT to be the integer satisfying $\lambda(NCT-1) < k < \lambda(NCT)$. Then

$$\begin{aligned} L(n) &= \sqrt{k^2 - (\lambda(n))^2}, && 0 \leq n \leq NCT-1 \\ -iL(n) &= \sqrt{(\lambda(n))^2 - k^2}, && n \geq NCT. \end{aligned} \tag{3.2}$$

The radial modes corresponding to $n=0,\cdots,NCT-1$ are called cuton, the other cutoff, and NCT is the number of cuton radial modes. Complex $R(n)$ is called the reflection coefficient of the n^{th} radial mode, while complex $A(n)$ is the strength of the forward propagating modes, since we assume that $A(n) = 0$ for $n \geq NCT$. This is a reasonable assumption since the plane of the 24 acoustic drivers of the SMS is about 13 duct interior diameters from S1.

Note that the dependence on m in the above notation has been suppressed.

The appropriate boundary value problem for the Helmholtz equation (the wave equation with the harmonic time dependence separated out) can be stated as follows:

Find ψ in class $C^2(\Omega) \cap C^1(\bar{\Omega})$ such that

$\Delta\psi + k^2 \psi = 0$ in Ω,

$$\frac{\partial \psi}{\partial \eta} = 0 \quad \text{on } S2, \tag{3.3}$$

ψ satisfies the radiation condition at infinity,

$\psi = \phi$ and $\frac{\partial \psi}{\partial \eta} = \frac{\partial \phi}{\partial \eta}$ on $S1$.

We use Helmholtz' formula (an application of Green's third identity) to convert (3.3) into an integral equation. Let $\underset{\sim}{x}$ denote the observation point and $\underset{\sim}{x}'$ the integration point. Then

(3.4)

$$\psi(\underset{\sim}{x}) \cdot \begin{cases} 4\pi, & \underset{\sim}{x} \in \Omega \\ 2\pi, & \underset{\sim}{x} \in S1 + S2 - (S1 \cap S2) \\ \pi, & \underset{\sim}{x} \in S1 \cap S2 \\ 0, & \underset{\sim}{x} \in D \end{cases}$$

$$= \int_{S1+S2} \left(\frac{\partial \psi}{\partial \eta'}(\underset{\sim}{x}') \frac{e^{ik\bar{R}}}{\bar{R}} - \psi(\underset{\sim}{x}') \frac{\partial}{\partial \eta'} \left(\frac{e^{ik\bar{R}}}{\bar{R}} \right) \right) dS',$$

where $\bar{R} = |\underset{\sim}{x} - \underset{\sim}{x}'|$. Here η' denotes the normal to $S1 + S2$ pointing into D. Now uniqueness for (3.3) implies that $\psi = \bar{\psi}(z,r)e^{im\theta}$. If we

change to cylindrical coordinates in (3.4), multiply by $e^{-im\theta}$, and integrate from $\theta = -\pi$ to $\theta = \pi$, we obtain the one-dimensional integral equation

(3.5)

$$\left.\begin{array}{ll} \bar{\psi}(z,r), & (z,r) \in C^2 - (C1 \cap C2) \\ \bar{\psi}(z,r)/2, & (z,r) = C1 \cap C2 \\ \bar{\phi}(z,r), & (z,r) \in C1 \end{array}\right\} = -\int_0^1 r' \, dr' \, \frac{\partial}{\partial z'} \bar{\phi}(0,r') \, K(z,r;0,r')$$

$$+ \int_0^1 r' \, dr' \, \bar{\phi}(0,r') \, \frac{\partial K}{\partial z'} (z,r;0,r')$$

$$- \int_{C2} r' \, ds' \, \bar{\psi}(z',r') \, \frac{\partial K}{\partial \eta'} (z,r;z',r'),$$

where

$$K(z,r;z',r') = \pi^{-1} \int_0^{\pi} \cos(mY) \, \frac{e^{ikR}}{R} \, dY, \tag{3.6}$$

$$R = \left[(z-z')^2 + (r-r')^2 + 4rr' \sin^2(Y/2)\right]^{1/2}, \tag{3.7}$$

s' denotes arc length on C2, and η' denotes the normal to C2 pointing toward the duct interior. We note that (3.5) appears to be homogeneous; however, $\bar{\phi}$ in (3.1) is the sum of two terms, one of which is assumed known. This is the excitation term

$$\sum_{n=0}^{\infty} A(n) e^{iL(n)z} \, J_m(\lambda(n)r)$$

controlled by the SMS.

4. THE NUMERICAL METHOD

Our numerical method is collocation. We require (3.5) to hold at specified (collocation) points on C1 + C2. We obtain a full, square complex linear system whose solution provides an approximate solution to (3.5).

For the approximation of $\overline{\phi}$ we truncate (3.1) at $n = N1 > NCT-1$,

$$\overline{\phi} \simeq \sum_{n=0}^{N1} \left(A(n)e^{iL(n)z} + R(n)e^{-iL(n)z}\right) J_m\left(\lambda(n)r\right). \tag{4.1}$$

To approximate $\overline{\psi}$ on C2, we first parameterize this contour. We will refer to certain values of this parameter t as knots. We require points B, C, D, E, and F to be knots. Additionally, knots are added so that BC is divided into K2 subintervals of equal length with respect to this parameter, CD into K3 subintervals, DE into K4 subintervals, and EF into K5 subintervals. This yields $N2 + 1 = K2 + K3 + K4 + K5 + 1$ knots.

An additional line segment AB can be added to the duct mouth and divided into K1 subintervals. This is useful if it is desired to alter the hardwall condition on AB. In the following $A = B$ and $K1 = \phi$, but activation of these parameters is provided for in our codes.

We use N2 Chapeau functions, $\overline{\psi}_n(s)$ depending on arc length s to approximate $\overline{\psi}$. These basis functions are centered at the values of s corresponding to the knots, except for the knot corresponding to the endpoint F of C2. This is because the solution at F must be zero for azimuthal mode index $m \geq 1$. Hence, we write

$$\overline{\psi} \simeq \sum_{n=N1+1}^{N1+N2} C(n)\, \overline{\psi}_n(s) \qquad \text{on C2.} \tag{4.2}$$

We have experimented with two numerical procedures.

I. (i) Collocate at $(0,r_0),\cdots,(0,r_{N1})$ where $0 < r_0 < \cdots < r_{N1} < 1$ satisfy $J_m\big(\lambda(N1+1)r_i\big) = 0$; i.e., choose the r coordinates to be positive zeros of the first term left out in the truncation (4.1) with $z = 0$.

(ii) Collocate at the points $(z_{N1+1},r_{N1+1}),\cdots,(z_{N1+N2},r_{N1+N2})$ corresponding to the centers of the Chapeau functions.

II. (i) as in I

(ii) as in I but replace the equation generated by the collocation point at B by the continuity equation

$$(4.3)\qquad -\sum_{n=0}^{N1} R(n)\, J_m\big(\lambda(n)\big) + C(N1+1) = \sum_{n=0}^{N1} A(n)\, J_m\big(\lambda(n)\big).$$

Now let $\underset{\sim}{R} = [R(0),\cdots,R(N1)]^T$, $\underset{\sim}{C} = [(N1+1),\cdots,C(N1+N2)]^T$, and $\underset{\sim}{A} = [A(0),\cdots,A(N1)]^T$. We write the linear system resulting from I or II by

$$(4.4)\qquad \text{CKTOT}*[\underset{\sim}{R},\underset{\sim}{C}]^T = \text{CRITE}*\underset{\sim}{A}\ ,$$

where CKTOT is a full, complex square matrix of order $N1 + N2 + 1$ and CRITE is an $(N1 + 1) \times (N1 + N2 + 1)$ complex matrix. Writing (4.4) in block form for procedure I we have

$$(4.5)\qquad \left[\begin{array}{c|c} \mathscr{A}+\mathscr{B} & \mathscr{C} \\ \hline \mathscr{E}+\mathscr{F} & \mathscr{D}+\mathscr{G} \end{array}\right]\left[\begin{array}{c} \underset{\sim}{R} \\ \hline \underset{\sim}{C} \end{array}\right] = \left[\begin{array}{c} \mathscr{B}-\mathscr{A} \\ \hline \mathscr{E}-\mathscr{F} \end{array}\right]\underset{\sim}{A}\ ,$$

where

$$\mathscr{A}(\ell,n) = J_m\big(\lambda(n) r_\ell\big), \qquad 0 \leq \ell,n \leq N1, \tag{4.6}$$

$$\left.\begin{array}{ll} \mathscr{B}(\ell,n), & 0 \leq \ell,n \leq N1 \\ \mathscr{C}(\ell,n), & N1+1 \leq \ell \leq N1+N2,\ 0 \leq n \leq N1 \end{array}\right\} \tag{4.7}$$

$$= -iL(n) \int_0^1 r'\, dr'\, J_m\big(\lambda(n) r'\big)\, K\big(z_\ell, r_\ell; 0, r'\big),$$

$$\mathscr{F}(\ell,n) = -\int_0^1 r'\, dr'\, J_m\big(\lambda(n) r'\big)\, \frac{\partial K}{\partial z'}\big(z_\ell, r_\ell; 0, r'\big), \tag{4.8}$$

$$N1+1 \leq \ell \leq N1+N2, \quad 0 \leq n \leq N1,$$

$$\left.\begin{array}{ll} \mathscr{E}(\ell,n), & 0 \leq \ell \leq N1, \quad N1+1 \leq n \leq N1+N2 \\ \mathscr{G}(\ell,n), & N1+1 \leq \ell,n \leq N1+N2 \end{array}\right\} \tag{4.9}$$

$$= \int_{C2} r'\, ds'\, \overline{\psi}_n(s')\, \frac{\partial K}{\partial \eta'}\big(z_\ell, r_\ell; z', r'\big),$$

$$\mathscr{D}(N1+1,\ N1+1) = 1/2$$

$$\mathscr{D}(\ell,\ell) \quad 1, \qquad N1+2 \leq \ell \leq N1+N2 \tag{4.10}$$

$$\mathscr{D}(i,j) = 0, \qquad N1+1 \leq i \neq j \leq N1+N2.$$

We note that $F(\ell,n) = 0$ for $0 \leq \ell \leq N1+1$ because $\frac{\partial K}{\partial z'}(0,r;0,r') = 0$ for $0 \leq r \neq r' \leq 1$.

If procedure II is used, then row N1 + 1 in CKTOT and CRITE must be changed according to the continuity equation (4.3).

The system (4.4) is solved NCT times with "basis" excitations $\underset{\sim}{A}_0,\cdots,\underset{\sim}{A}_{NCT-1}$ which satisfy $\underset{\sim}{A}_j(i) = \delta_{ij}$. We call the resulting approximate solutions to (3.5), basis approximate solutions and denote them by $\underline{\phi}^i$ and $\underline{\psi}^i$.

Calculation of the basis far field (or basic first Neumann iterate) is done using the Helmholtz' formula:

$$(4.11)\qquad F^i(z,r) \cdot \begin{cases} 2, & (z,r,\theta) \text{ in } \Omega \\ 1, & (z,r) \in C1 + C2 - (C1 \cap C2) \\ 1/2, & (z,r) = C1 \cap C2 \end{cases}$$

$$= -\int_0^1 r' \, dr' \, \frac{\partial \underline{\phi}^i}{\partial z'}(0,r') \, K(z,r;0,r')$$

$$+ \int_0^1 r' \, dr' \, \underline{\phi}^i(0,r') \, \frac{\partial K}{\partial z'}(z,r;0,r')$$

$$- \int_{C2} r' \, ds' \, \underline{\psi}^i(z',r') \, \frac{\partial K}{\partial \eta'}(z,r;z',r').$$

Given the coefficients $A(0),\cdots,A(NCT-1)$ of the desired excitation, we find the corresponding approximate solution to (3.5) and the far field (or first Neumann iterate) from

$$(4.12)\qquad \underline{\phi} = \sum_{i=0}^{NCT-1} A(i)\underline{\phi}^i, \quad \underline{F} = \sum_{i=0}^{NCT-1} A(i)\underline{F}^i.$$

The initial choice of N1 and N2 in (4.1) and (4.2) may not always be consistent with the desired accuracy. Also, the equispacing of the knots with

respect to the parameter t is usually suboptimal. Section 6 discusses rules for choosing N1 and N2 initially. We now present a procedure (see [deBoor2]) which uses the first approximate solution obtained to estimate the absolute error at the knots, and then recommends new values for K2, K3, K4 and K5 and a new distribution of the knots. The goal being to equally distribute the absolute error among the knots and to achieve a desired accuracy.

Let us explain this procedure for BC which is initially divided into K2 subintervals. Let t_i denote an interior knot and let h_i and h_{i+1} denote the mesh spacing immediately to the left and right of t_i. Set $h = \max\{h_i, h_{i+1}\}$. At t_i we estimate the second derivative with respect to t of the j^{th} basis approximate solution to (3.5) by interpolation with a parabola at t_{i-1}, t_i and t_{i+1}. Denote this estimate by d_i^j and set $d_i = \max\{|d_i^j|: 0 \leq j \leq NCT-1\}$. We estimate the absolute error at t_i by $d_i h^2/2$. Let AE denote the sum of the errors at the interior knots divided by the number of interior knots, K2-1. Let AER denote the desired absolute error, and set

$$L2 = \left[K2/\sqrt{AER/AE}\right] + 1,$$

unless the result is 1, in which case set L2 = 2.

Next, we partition BC into L2 subintervals so that the error is approximately the same at all interior knots. Set p = K2 and ℓ = L2 and let $t_1, \cdots, t_{p+1}$ denote the initial knots on BC. Set $u_1 = t_1$, $u_i = (t_i + t_{i+1})/2$, $i = 2, \cdots, p-1$, $u_p = t_{p+1}$. Let G denote the piecewise constant function defined by $G(t) = \sqrt{d_{i+1}}$ for $u_i < t < u_{i+1}$. For $u_1 \leq u \leq u_p$, define

$$y = \int_{u_1}^{u} G(t)dt \qquad \text{and} \qquad y_p = \int_{u_1}^{u_p} G(t)dt.$$

Now y is increasing in u so let $u = H(y)$ denote the inverse function. Construct $\ell + 1$ new knots according to $\omega_1 = t_1$, $\omega_i = H\big((i-1)y_p/\ell\big)$, $i = 2,\cdots,\ell$, $\omega_{\ell+1} = t_{p+1}$. This procedure is based on our observation that in this problem the redistribution of a fixed number of knots has little effect on the average error AE.

5. CODE DESCRIPTION

We will discuss the following codes: CLLEQS (CLLIQS), CLLRDS (CLLIRS), NELMAN, FALFLD, and SPDATA. CLLEQS use the continuity condition (4.3) at C1 C2, while CLLIQS and CLLIRS collocate at this point. Our codes are programmed in CDC Fortran 5 (Fortran 77).

We begin by discussing CLLIQS. First, values for $k = \overline{ka}$ (RKA), m, N1, N2, NCT, and AER, the error tolerance for C2, must be input. CLLIQS contains the data $X(0),\cdots,X(N1MAX)$, $\lambda(0),\cdots,\lambda(N1MAX)$ in arrays ZERO and RLAMDA for $m = 1,\cdots,4$ (currently), where $J_m(X(i)) = 0$ and $J_m'(\lambda(i)) = 0$. Array RL contains the complex parameters $L(0),\cdots,L(N1MAX)$. Currently, N1MAX = 13. The value of NCT, the number of cuton modes is computed from RLAMDA and k, and then checked against the user supplied value.

Subroutine CURV contains the parameterization of C2 and provides, for a given parameter value t, the corresponding value of z and r, the z and r components of the normal, and the value of arc length measured from B. The values of the constants determining the location of B, C, D, E and F are stored in subroutine CONSTS.

BC is an arc of the ellipse in the z-r plane given by

$$\left(\frac{z}{.4161438}\right)^2 + \left(\frac{r - 1.2080719}{.2080719}\right)^2 = 1,$$

which joins B = (0,1) to C = (.147804, 1.4025775). CD is the line segment joining C to D = (-1.6187892, 1.7381843). DE is the line segment joining D to E = (-2.6, 1.7381843), and EF is an arc of a circle of radius 1.7381843 with center (-2.6, 0) joining E and F = (-4.3381843, 0).

Arc length on BC is computed by approximating

$$S(t) = .4161438 \int_0^t \sqrt{(5 + 3\cos(2\tau))/8}\, d\tau$$

using 10 point, piecewise cubic Hermite interpolation for $0 \leq t \leq 2.7784911$. This is accomplished in subroutine HERM and BARCL.

Subroutine KNOTGN generates the knots (array RKNOT) on C2 in terms of the parameter t as described in Section 4. Subroutine COLLGN uses CURV and KNOTGN to produce the N1+N2+1 collocation points (arrays COLLZ, COLLR) and the values of arc length corresponding to the knots (array ARCL).

Subroutine COEFF assembles the complex matrices CKTOT and CRITE in (4.4). Almost all the execution time of CLLIQS is devoted to this one subroutine. The difficulty is that the oscillatory and singular double integrals in (4.7) - (4.9) must be computed. We use adaptive integration which is ideal for this type of behaviour, but expensive. We were constrained by the need to test our formulation and produce a working code during 14 weeks at ICASE in the summer of 1982. Alternatively, we could have developed a suitable product integration formula and then used the Nystrom method instead of collocation, but this would have required more time.

We have separated the integrands in (4.7) - (4.9) into a bounded part and a singular part corresponding to the axisymmetric potential equation.

Let $\rho = \left((r'-r_\ell)^2 + (z'-z_\ell)^2\right)^{1/2}$ and $\bar{\rho} = \left((r'+r_\ell)^2 + (z'-z_\ell)^2\right)^{1/2}$, let $\zeta = kR/2$, $\eta' = (N_{z'}, N_{r'})$, and let $\mathscr{K}$ and $\mathscr{E}$ denote the complete elliptic integrals of the first and second kinds as functions of the complementary parameter $m_1 = \rho^2/\bar{\rho}^2$.

Then in (4.7) we have

$$\mathscr{B}(\ell,n) = -\frac{iL(n)}{\pi}\int_0^1 r'\,dr'\,J_m(\lambda(n)r')\int_0^\pi dY\left(\cos(mY)(e^{ikR}-1) + \cos(mY)-1\right)/R$$

$$-\frac{iL(n)}{\pi}\int_0^1 r'\,dr'\,J_m(\lambda(n)r')\int_0^\pi \frac{dY}{R}$$

$$= -\frac{iL(n)k}{\pi}\int_0^1 r'\,dr'\,J_m(\lambda(n)r')\int_0^\pi dY\left(i\cos(mY)\sin(\zeta)e^{i\zeta} - \sin^2(mY/2)\right)/\zeta$$

$$-\frac{2iL(n)}{\pi}\int_0^1 r'\,dr'\,J_m(\lambda(n)r')\,\mathscr{K}(m_1)/\bar{\rho}\ ,$$

while in (4.9) we have

$$\mathscr{C}(\ell,n) = \pi^{-1}\int_{C2} r'\,ds'\,\bar{\psi}_n(s')\int_0^\pi dY\left(\cos(mY)\frac{\partial}{\partial\eta'}\left(\frac{e^{ikR}-1}{R}\right) + \left(\cos(mY)-1\right)\frac{\partial}{\partial\eta'}\frac{1}{R}\right)$$

$$+\pi^{-1}\int_{C2} r'\,ds'\,\bar{\psi}_n(s')\int_0^\pi dY\,\frac{\partial}{\partial\eta'}\frac{1}{R}$$

$$= \frac{k^2}{2\pi}\int_{C2} r'\,ds'\,\bar{\psi}_n(s')\int_0^\pi dY\left(N_{z'}(z'-z_\ell)+N_{r'}\left(r'-r_\ell + 2r_\ell\sin^2(Y/2)\right)\right)$$

$$\cdot\left\{i\cos(mY)e^{i\zeta}\left(\frac{\zeta\cos\zeta - \sin\zeta}{\zeta^2} + i\frac{\sin\zeta}{\zeta}\right) + \left(\frac{\sin(mY/2)}{\zeta}\right)^2\right\}$$

$$+ \pi^{-1} \int_{C2} ds' \frac{\overline{\psi}_n(s')}{\overline{\rho}}$$

$$\cdot \left\{ 2r' \mathscr{E}(m_1) \left(N_{r'}(r_\ell - r') + N_{z'}(z_\ell - z') \right) / \rho^2 + N_{r'} \left(\mathscr{E}(m_1) - \mathscr{K}(m_1) \right) \right\} .$$

For the evaluation of J_1, J_m, $m \geq 2$, $\mathscr{K}(m_1)$ and $\mathscr{E}(m_1)$ we use the LRC FTN5MLB library routines BJ1R, BKIR, ELIPKC and ELIPEC. For the evaluation of the one-dimensional integrals we use the FTN5MLB routine CADRE which is a modification of an algorithm due to deBoor [deBoor1]. For the double integrals we use the FTN5MLB routine CAREDB which computes the integral as iterated single integrals with the single integrals computed as in CADRE.

CADRE is an adaptive cautious Romberg extrapolation routine which is designed to identity certain types of integrand behaviour by examining a ratio based on the previous three trapezoidal sums. We split the integrals so that the singularities are endpoint singularities. If such a singularity is detected, CADRE switches to a process similar to Aitken's δ^2 process to estimate the integral and evaluate the error. As a result of this switching, we have observed that execution times decrease with the error tolerances. We use EPS(1) = EPS(2) = E-5, where EPS(1) is the maximum allowable relative error and EPS(2) the maximum allowable absolute error. EPS(3) is the sum of the computed error estimates over each subinterval in which the convergence criteria is satisfied. These remarks also hold for CAREDB.

Adaptive integration is particularly suited to oscillatory and (or) singular integrals. It offers the possibility of constructing a test code for an integral equation method in a relatively short time. Both CADRE and CAREDB require real integrands so real and imaginary parts were integrated separately. We did not take the time to convert these routines into integrators for complex valued functions.

Once the linear system (4.4) is assembled, we solve it using FTN5MLB routine CXGCOIT. This subroutine performs an LU decomposition, solves by forward and backward substitution, and estimates the condition number (CONDNUM) of CKTOT in the 1-norm. Optionally, iterative refinement can be performed (see [Don]).

Finally, recommended values for K2, K3, K4 and K5, with respect to an absolute error tolerance (AER) on C2 are computed, and estimates made of the second derivative of the approximate solution (with respect to the parameter t) at the interior knots of BC, CD, DE and EF.

On execution a listing is provided of all input parameters, NCT, RLAMDA, ZERO, COLLZ, COLLR, RKNOT, ARCL, CONDNUM, the real and imaginary parts of the complex approximate solution (as well as phase and amplitude), a continuity check at C1 $\cap$ C2, recommended values for K2, K3, K4, K5, and estimates of second derivatives and error on C2. In addition, the maximum integration error estimate and the corresponding indices is written for the matrices $\mathscr{B}$ and $\mathscr{E}$, for $\mathscr{F}$, and for $\mathscr{L}$ and $\mathscr{G}$.

Program CLLRDS is essentially the same as CLLEQS except that provision is made in subroutine KNOTGN for using the recommended values of K2, K3, K4, K5 and the second derivative estimates to distribute this new number of knots.

Program NELMAN takes the output of CLLEQS, CLLIQS, CLLRDS or CLLIRS and computes one basis Neumann iterate. This iterate and corresponding integration error estimates are output.

Program FALFLD takes the output of CLLEQS, CLLIQS, CLLRDS, CLLIRS or NELMAN and computes an approximate basis far field. The basis far field and corresponding integration error estimates are output.

Program SPDATA takes the output of FALFLD and user provided excitation data $A(0),\cdots,A(NCT-1)$ (amplitude in dB, phase in degrees) and computes and outputs the approximate solution and far field. The far field amplitude is referenced to its maximum value. Finally, plotting files are created.

6. NUMERICAL RESULTS

All computations were performed on a CDC Cyber 175 at NASA Langley Research Center. We give results for the programs which collocate at $C1 \cap C2$ instead of demanding the continuity equation (4.3) hold. We have found little difference in the outputs of these two sets of programs.

For a given azimuthal mode index m, it is best to start with a value of $k = \overline{ka}$ so that one mode is cuton (NCT = 1) and then increase k to the desired level. Good starting values then are $N1 = NCT + 5$ and $K2 = 20$, $K3 = 10$, $K4 = 10$, $K5 = 7$. Program CLLIQS recommends new values for $K2,\cdots,K5$ with respect to a user supplied tolerance. The user has the option of running CLLIRS with these new values and derivative estimates from CLLIQS as input. We have provided a continuity check which outputs the modulus of the difference in the two sides of (4.3) for an approximate solution. If this continuity check is greater than the error tolerance, then N1 can be increased in CLLIRS.

The error estimates on C2 and the continuity check are a reasonable indication of the accuracy attained. Of course, the condition number and the accuracy with which CKTOT and CRITE are computed must also be considered. We have run CLLIRS for $k = \overline{ka} = 2.66$ and an increasing sequence of values for $N1 + N2$. Table I gives some of these results. CONT is the value of the

continuity check. The error in $|R(0)|$ and the error at $C1 \cap C2$ are estimated by comparison with the case $N1 + N2 = 78$. These data support the hypothesis that the condition number in the 1-norm satisfies

$$\text{CONDNUM} \lesssim 1.8\ N1 + 4.5\sqrt{N2}\ ,$$

and that the error in $R(0)$ and the maximum error on $C2$ are less than

$$\max\left\{\frac{K_1}{2^{N1}}\ ,\ \frac{K_2}{(N2)^2}\right\}$$

for some constants K_1 and K_2.

Table II gives for $m = 1$ a comparison of experimental and numerical results. Some of these results are in close agreement; for example, for $k = 2.66$, we have $|R(0)|/|A(0)| = .348$ (numerical) and .35 (experimental). However, for $k = 3.20$, we have $|R(0)|/|A(0)| = .164$, while the experimental value is .196. Our error tolerance here is .002. The continuity check and error estimates on $C2$ are consistent with this tolerance. Generally, when $R(i)$ is small compared to $\max\{|A(0)|,\cdots,|A(NCT-1)|\}$, we have the greatest relative error. We have indicated the error bracket on some of these entries in Table II. But these brackets do not account for some of the discrepancies. We note that the dB levels in Table II are referenced so that the peak sound pressure level in the far field is 0 dB (for both experimental and numerical results).

Figures 3, 4, 5, 6, and 7 give far field patterns computed on a semicircle of radius 20 in front of the duct (see Figure 1). We note the good agreement between the numerical and experimental curves. The small oscillations in the

experimental curve may be due to reflections, while the lack of symmetry indicates less than complete isolation of the desired azimuthal mode. We compute and store a basis approximate solution and far field. Then we can interactively produce approximate solutions and far field patterns for any given excitation strengths $A(0),\cdots,A(NCT-1)$. Thus we have an NCT parameter family of possible far fields that can be generated quickly. It is possible, for example to make the -30 dB downward spikes in the $k = 6.50$ case almost completely disappear by choice of excitation strengths. But roughly speaking, these different patterns have the same "envelope."

7. REMARKS

We will discuss existence, uniqueness and regularization in detail in a later report. For now we note that the standard proof using a theorem of Rellich (see, i.e., [Hellwig]) shows that uniqueness holds for the boundary value problem (3.3). On the other hand uniqueness may not hold for the integral equation (3.5). If uniqueness does not hold for (3.5), it follows that k is an eigenvalue for Helmholtz' equation in the interior of $S1 + S2$ with Dirichlet boundary conditions, and that the corresponding eigenfunction has the form $u(z,r)e^{im\theta}$. If k is such an eigenvalue, we have not been able to adapt the usual method to produce a homogeneous solution to (3.5). However, the numerical evidence, namely the variation of conditioning with changes in k suggests that nonuniqueness does hold at such interior eigenvalues.

We have considered the problem of regularizing (3.5). A good discussion of this problem can be found in [Burton] and the references there. We have

developed a regularization procedure based on a vector relationship due to Maue (see [Burton]). This procedure uses the Galerkin method, Maue's formula and Stokes' theorem to move a derivative from the kernel to the unknown function. This reduces the strength of the singularity which must be integrated. This procedure has not yet been fully implemented and tested. Our current code provides condition number estimates, a continuity check (when collocation is used at $C1 \cap C2$), and error estimates on C2. These should indicate when the results are unreliable.

We have experimented with the best location for the interface surface S1. This is a trade-off between the two types of approximation - Bessel series and piecewise linear splines. The best efficiency is obtained by using the modal expansion over as large a region as possible.

We have already mentioned the idea of a full engine model. This more complex geometry would be stored in subroutine CURV. Two interface surfaces and two modal expansions would be required. This is a natural extension of the current code. It is also possible to install a variable geometry. The input would be points on the outer duct contour and the code would automatically connect these points with a smooth curve having some specified property.

In conclusion we point out that duct acoustics has been studied extensively in recent years. The reader is referred to [Baum] for a bibliography and a discussion of the various numerical methods which have been used.

REFERENCES

[Abram] Abramowitz, M. and Stegun, I. A., Handbook of Mathematical Functions, NBS Applied Mathematics Series 55, U.S. Government Printing Office, 1972.

[Baum] Baumeister, K. J., Numerical Techniques in Linear Duct Acoustics - 1980-81 Update, NASA Technical Memorandum 82730, 1981.

[Burton] Burton, A. J., Numerial solution of scalar diffraction problems, Chapter 21 in Numerical Solution of Integral Equations by Delves.

[deBoor1] de Boor, C., CADRE: Algorithm for numerical quadrature, Chapter 7 in Mathematical Software, John R. Rice, ed., Academic Press, 1971.

[deBoor2] de Boor, C., CADRE: A Practical Guide to Splines, Springer-Verlag, 1978.

[Don] Dongarra, J. J., Bunch, J. R., Moler, C. B., and Stewart, G. W., LINPACK User's Guide, SIAM, 1979; Technical Memorandum No. 313, Applied Mathematics Division, Argonne National Laboratory, Argonne, IL, August 1977.

[Hamdi] Hamdi, M. A., Une formulation variationnelle par equations integrales pour la resoluton de l'equation de Helmholtz avec des conditions aux limites mixtes, Compte Rendu a l'Academie des Sciences de Paris, 292, Serie II, 1981, pp. 17-20.

[Hellwig] Hellwig, G., Partial Differential Equations, Blaisdell Publishing Company, New York, 1964.

[Kag] Kagawa, Y., Yamabuchi, T., Yoshikawa, T., Ooie, S., Kyouno, N., and Shindou, T., Finite element approach to acoustic transmission-radiation systems and application to horn and silencer design, J. Sound Vibration, 69 (2), 1980, pp. 207-228.

[Meyer] Meyer, W. L., Bell, W. A., Zinn, B. T., and Stallybrass, M. P., Boundary integral solutions of three-dimensional acoustic radiation problems, J. Sound Vibration, 59 (2), 1978, pp. 245-262.

[Pal] Palumbo, D. L., An Operations Manual for the Spinning Mode Synthesizer in the Langley Aircraft Noise Reduction Laboratory, NASA Contractor Report 165698, 1981.

[Ship] Shippy, D. J., Rizzo, F. J., and Gupta, A. K., Boundary-integral solution of potential problems involving axisymmetric bodies and nonsymmetirc boundary conditions, Developments in Theoretical and Applied Mechanics, 10, 1980, pp. 189-206.

[Silcox] Silcox, R. J., Experimental Investigation of Geometry and Flow Effects on Acoustic Radiation from Duct Inlets, AIAA-83-0713, 1983.

[Ville] Ville, J. M. and Silcox, R. J., Experimental Investigation of the Radiation of Sound from an Unflanged Duct and a Bellmouth Including the Flow Effect, NASA TP-1697, 1980.

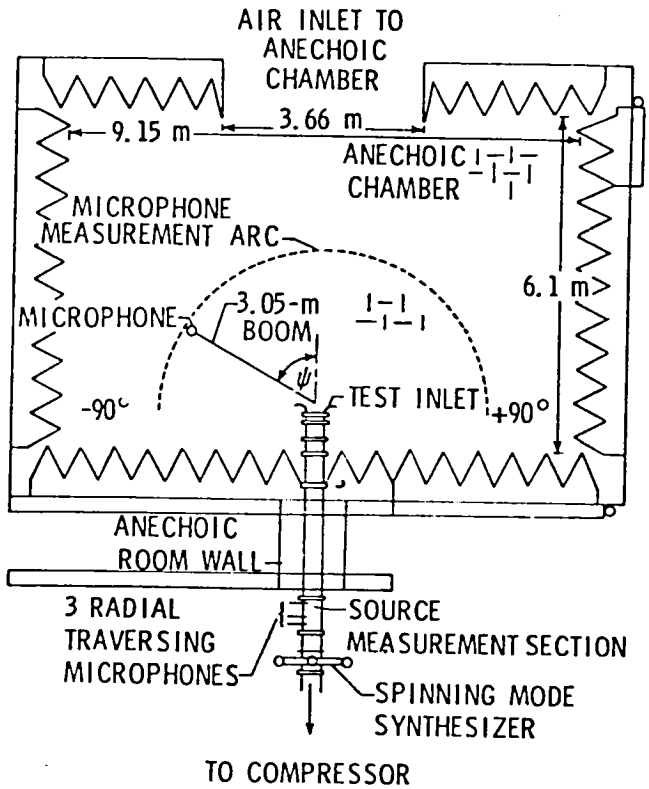

Figure 1. Plan view of SMS/flow duct facility in Aircraft Noise Reduction Laboratory

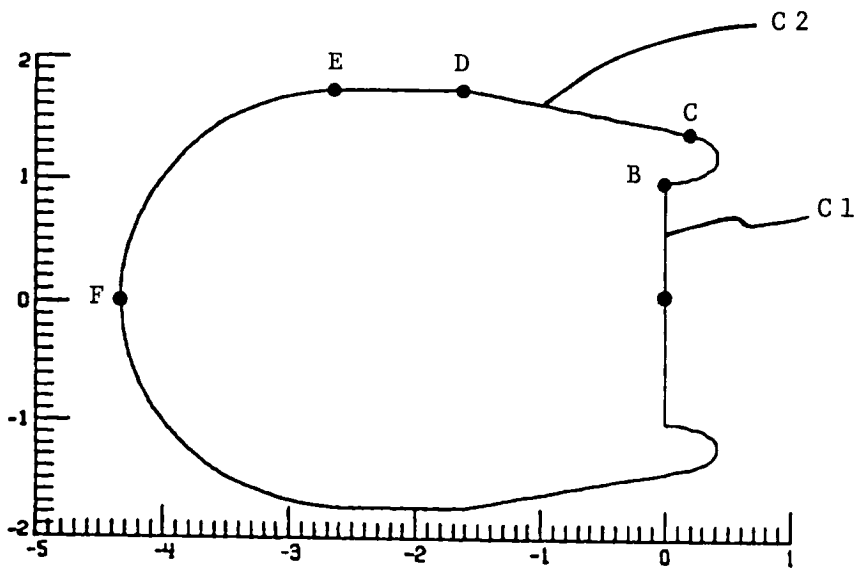

Figure 2

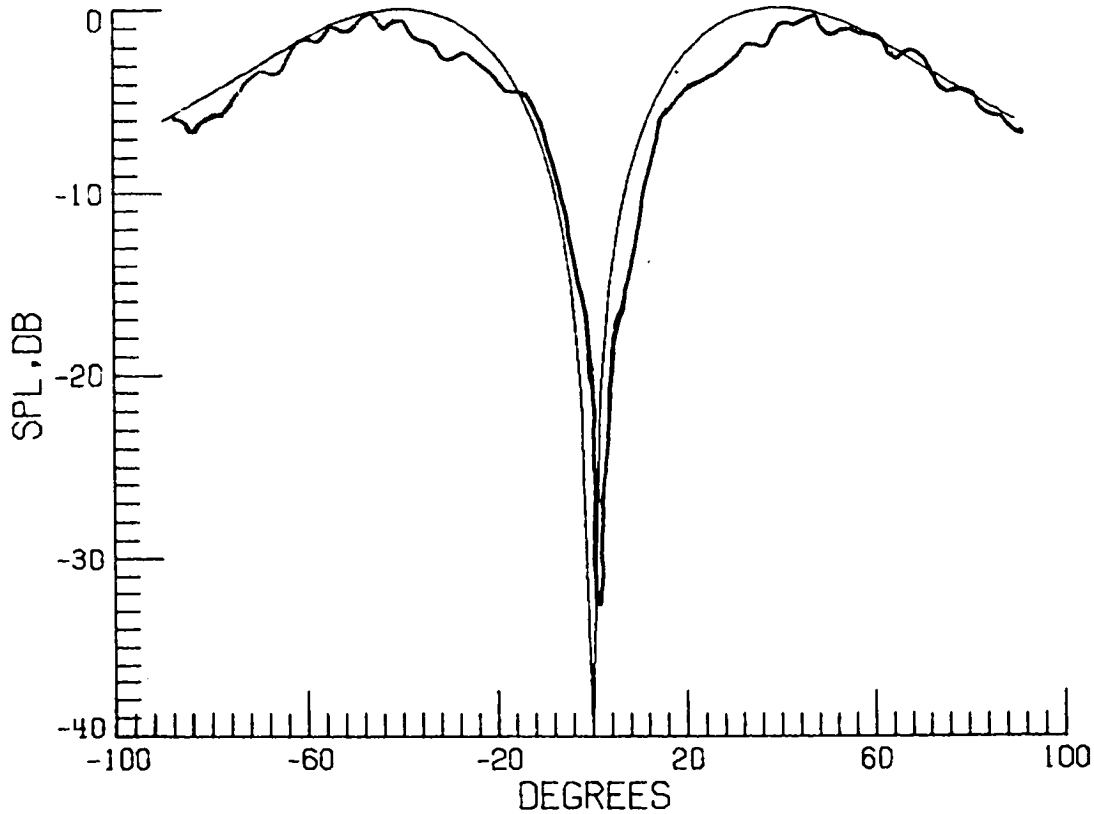

Figure 3. **m = 1, k = 2.66, NCT = 1.**

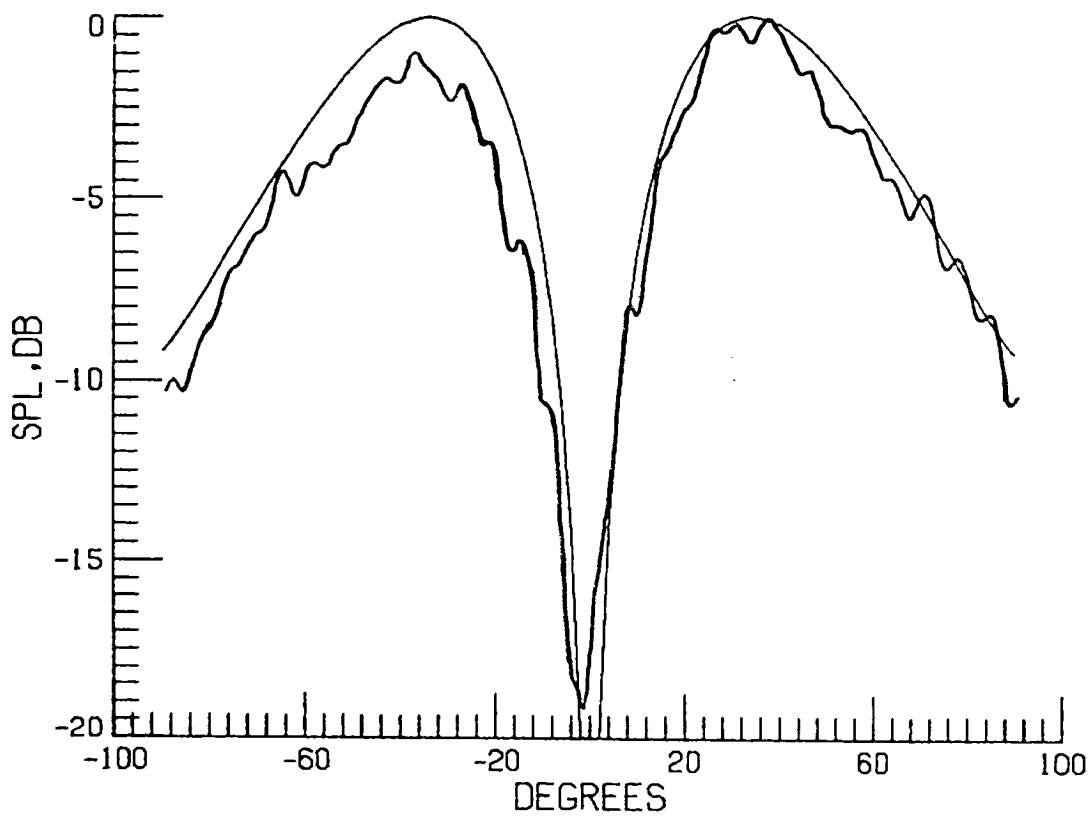

Figure 4. m = 1, k= 3.20, NCT = 1.

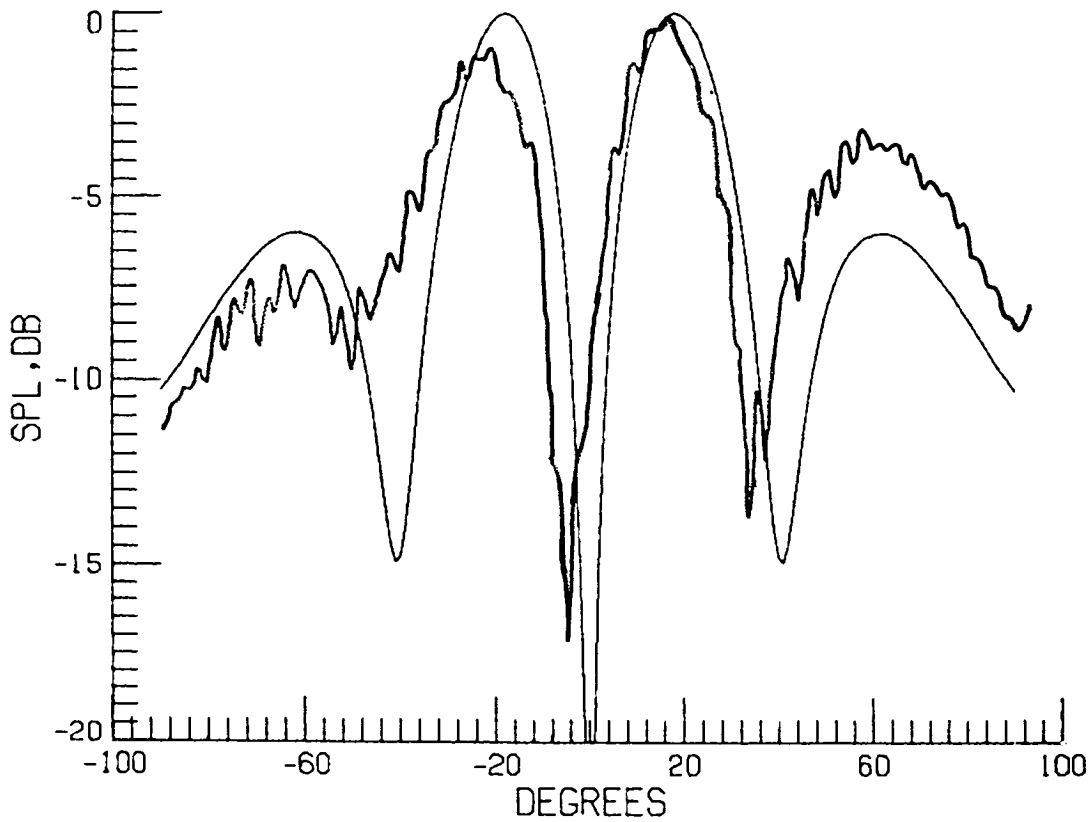

Figure 5. m = 1, k = 5.54, NCT = 2.

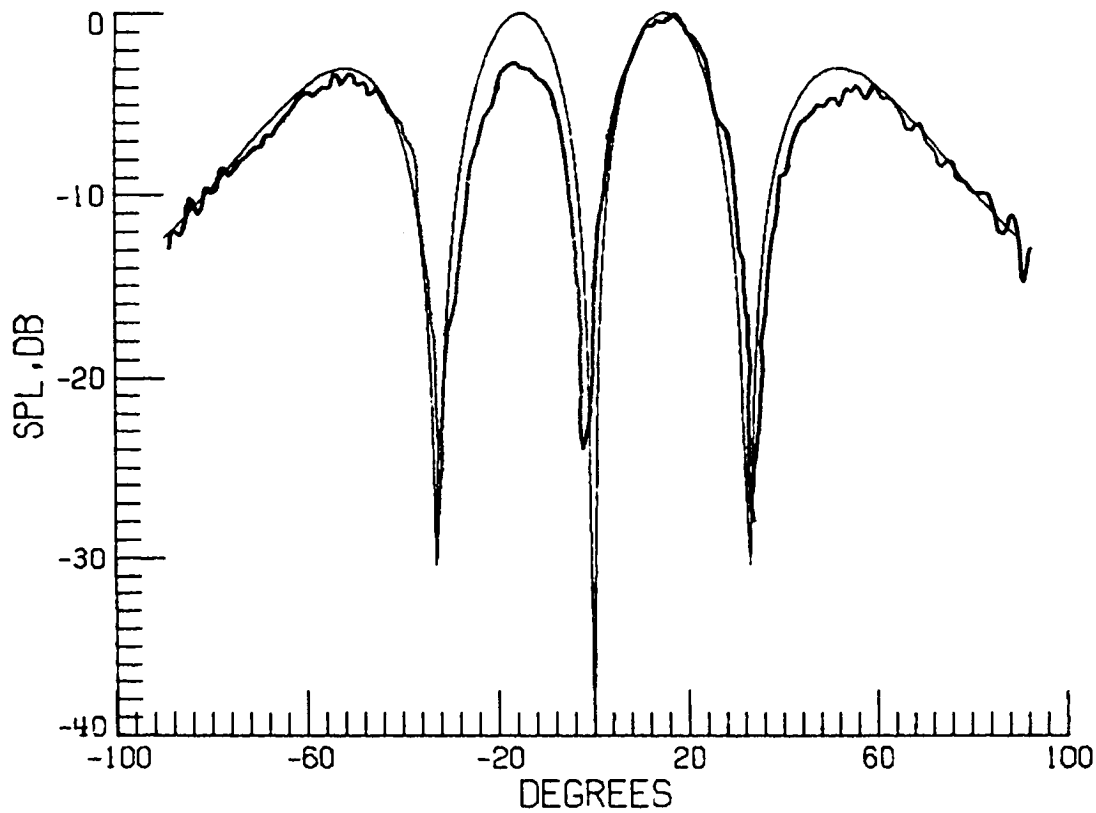

Figure 6. m = 1, k = 6.50, NCT = 2.

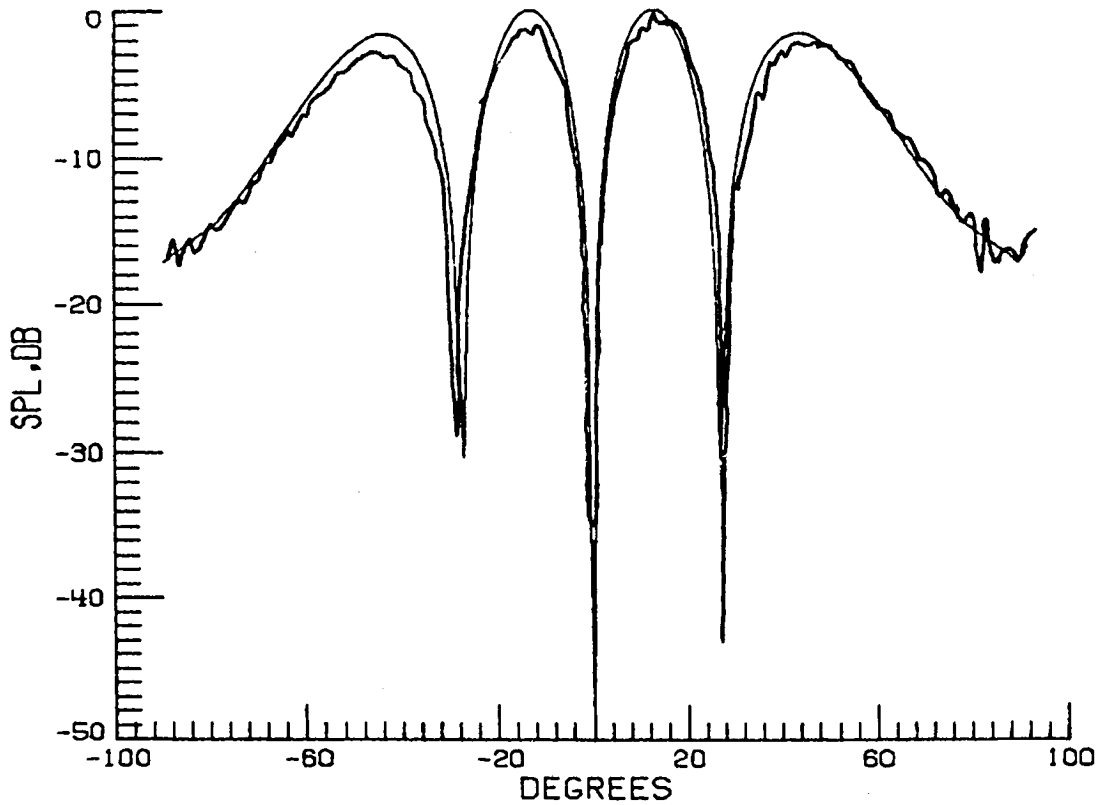

Figure 7. m = 1, k = 7.68, NCT = 2.

Table I

N1	N2	CONDUM	CONT	|R(0)|	ANGLE R(0)	ERROR |R(0)|	ERROR C1 ∩ C2	MAX ERROR EST. C2
6	18	29	.0016	.3555	-20.76	.011	.0077	.0080
2	34	26.8	.006	.3479	-20.13	.0029	.0012	.0021
6	34	34.1	.00076	.3476	-20.17	.0027	.0015	.0019
10	34	41.2	.00044	.3475	-20.17	.0026	.0019	.0019
6	68	47.9	.0011	.3451	-20.00	.000043	.00037	.00051
10	68	54.2	.00038	.3451	-20.00			

Table II. Max Far Field SPL = 0 dB

NUMERICAL				EXPERIMENTAL
$k = \overline{ka}$	Coefficient	dB	Angle	dB
2.66	A(0)	36.0	0^o	36.1
	R(0)	26.8	-20.2^o	27.0
3.20	A(0)	33.8	0^o	32.6
	R(0)	$18.1 \pm .2$	25.2^o	18.5
5.54	A(0)	24.4	-8.4^o	25.8
	R(0)	2.2 ± 1.64	29.8^o	18.3
	A(1)	37.8	-139.1^o	39.2
	R(1)	28.5	141.3^o	29.6
6.50	A(0)	23.9	70.4^o	22.9
	R(0)	-9.2 ± 4.3	19.90^o	9.9
	A(1)	34.5	-64^o	33.5
	R(1)	-1.3 ± 1.7	-54^o	9.9
7.68	A(0)	23.4	-159.6^o	23.5
	R(0)	-5.4 ± 2.2	-168.2^o	3.4
	A(1)	33.0	56.6^o	33.1
	R(1)	-4 ± 1.2	-5.7^o	9.5

1. Report No.	2. Government Accession No.	3. Recipient's Catalog No.
NASA CR-172273		

4. Title and Subtitle	5. Report Date
Spinning Mode Acoustic Radiation From The Flight Inlet	November 1983
	6. Performing Organization Code

7. Author(s)	8. Performing Organization Report No.
William F. Moss	83-63
	10. Work Unit No.

9. Performing Organization Name and Address	11. Contract or Grant No.
Institute for Computer Applications in Science and Engineering Mail Stop 132C, NASA Langley Research Center Hampton, VA 23665	NAS1-16394, NAS1-17130
	13. Type of Report and Period Covered
12. Sponsoring Agency Name and Address National Aeronautics and Space Administration Washington, D.C. 20546	contractor report
	14. Sponsoring Agency Code

15. Supplementary Notes

Langley Technical Monitor: Robert H. Tolson
Final Report

16. Abstract

A mathematical model has been developed for spinning mode acoustic radiation from a thick wall duct without flow. This model is based on a series of experiments (with and without flow) conducted by Richard Silcox [Silcox] of the Noise Control Branch at Langley Research Center. In these experiments a nearly pure azimuthal spinning mode was isolated and then reflection coefficients and far field pressure (amplitude and phase) was measured. In our model the governing boundary value problem for the Helmholtz equation is first converted into an integral equation for the unknown acoustic pressure over a disk, S1, near the mouth of the duct and over the exterior surface, S2, of the duct. Assuming a pure azimuthal mode excitation, the azimuthal dependence is integrated out which yields an integral equation over the generator C1 of S1 and the generator C2 of S2 (see Figure 2). We approximate the sound pressure on C1 by a truncated modal expansion of the interior acoustic pressure. We use piecewise linear spline approximation on C2. We collocate at the knots of the spline and at zeros of the first term excluded in the truncated modal expansion. Finally, we compare numerical and experimental results.

17. Key Words (Suggested by Author(s))	18. Distribution Statement
acoustic radiation integral equations numerical solution	64 Numerical Analysis 71 Acoustics Unclassified-Unlimited

19. Security Classif. (of this report)	20. Security Classif. (of this page)	21. No. of Pages	22. Price
Unclassified	Unclassified	32	A03

For sale by the National Technical Information Service, Springfield, Virginia 22161

NASA-Langley, 1984